ingegneria sismica
International Journal of Earthquake Engineering
Anno XLIII - Num. 2 - 2026

# Edge computing supports the design of real-time monitoring and dynamic prediction system for soil erosion

*Lei Lei*[1,*], *Chenxi Wang*[2], *Hongmei Cai*[1], *Dong Zhang*[3], *Yusheng Zhang*[2] *and Qingyun Chen*[1]

[1] State Grid (Xi'an) Environmental Protection Technology Center Co., Ltd., Xi'an 710100, Shaanxi, China
[2] Electric Power Research Institute of State Grid Shaanxi Electric Power Co., Ltd., Xi'an 710100, Shaanxi, China
[3] State Grid Shaanxi Electric Power Co., Ltd., Xi'an 710048, Shaanxi, China

**SUMMARY:** *Soil erosion is one of the major ecological and environmental problems affecting watershed security, agricultural productivity, and the sustainable utilization of land resources. Under the combined influence of extreme weather events, land-use change, and human disturbance, the spatiotemporal evolution of soil erosion has become increasingly complex, creating an urgent need for accurate real-time monitoring and dynamic prediction. Traditional soil erosion monitoring methods mainly rely on field surveys, remote sensing interpretation, hydrological modeling, and centralized cloud-based data processing. Although these approaches provide important support for regional erosion assessment, they still suffer from low temporal resolution, delayed response, high communication overhead, limited local adaptability, and insufficient real-time early-warning capability in complex environments. In particular, when massive multi-source sensor data must be processed continuously, centralized architectures often encounter bottlenecks in latency, bandwidth consumption, and system robustness. To address these problems, this study proposes an edge-computing-supported dynamic prediction system for real-time soil erosion monitoring. The system integrates Internet of Things sensing devices, edge nodes, wireless communication networks, and a cloud-edge collaborative architecture to achieve efficient acquisition, transmission, analysis, and feedback of erosion-related data. Multi-dimensional indicators, including rainfall intensity, soil moisture, runoff status, vegetation coverage, slope-related terrain information, and surface sediment changes, are collected in real time through distributed sensing units. Edge nodes perform data cleaning, feature extraction, local fusion, and preliminary prediction near the data source, thereby reducing transmission pressure and improving response efficiency. On this basis, a dynamic prediction model combining temporal sequence analysis, spatial factor fusion, and intelligent learning algorithms is constructed to identify erosion risk levels and predict erosion trends under changing environmental conditions. A visualization and warning module is further designed to display monitoring results, risk distribution, and temporal evolution characteristics intuitively. Experimental results based on 12 monitoring points and 328,000 valid records from measured and simulated scenarios show that the proposed system achieves an average response time of 1.12 s, which is 31.4% lower than that of the traditional centralized processing mode. The proposed prediction model reaches an Accuracy of 95.8% and an F1-score of 95.3% on the test set, showing clear advantages in monitoring timeliness, prediction accuracy, and operational stability. The study provides a feasible technical framework for intelligent soil and water conservation, disaster prevention, and ecological management, and offers practical*

*shuibaozu@163.com
https://doi.org/10.65102/is2026785
Published: 30 April, 2026

*support for the digital and intelligent development of soil erosion monitoring systems.*

***KEYWORDS:*** *Soil erosion; Edge computing; Real-time monitoring; Dynamic prediction; Intelligent warning*

# 1 Introduction

With the continuous improvement of the digital level of ecological governance, soil and water loss monitoring is shifting from stage investigation to continuous perception and dynamic judgment. As an important environmental problem affecting watershed ecological security, cultivated land quality maintenance and infrastructure stability in mountainous areas, soil and water loss is jointly affected by multiple factors such as rainfall intensity, slope morphology, soil moisture content, vegetation cover change and human disturbance, and its formation mechanism has significant spatio-temporal coupling characteristics [1]. Traditional monitoring methods mostly rely on manual inspection, remote sensing interpretation, fixed-point hydrological observation and centralized data processing platform. Although they can provide basic support for regional erosion investigation and governance assessment, there are still obvious shortcomings in monitoring frequency, field response, heterogeneous data fusion and rapid identification of local risks. It is difficult to adapt to the application requirements of real-time monitoring and dynamic early warning under complex surface conditions [2, 3].

In recent years, scholars at home and abroad have carried out a wealth of research on soil erosion identification, erosion sensitivity assessment and gully erosion risk prediction. Most of the related works abroad use machine learning, remote sensing inversion and geostatistical analysis methods to model the coupling relationship of erosion factors, the spatial susceptibility partition and the geomorphological evolution process. Domestic research has made rapid progress in ditch erosion identification, erosion grade discrimination and multi-source environmental factor analysis in the scenes of Loess Plateau, Northeast black soil region and typical small watershed [4, 5]. At the same time, the development of iot perception, wireless transmission and edge computing provides a new implementation path for ecological environment monitoring system [6]. Some studies on agricultural environment and irrigation management show that deploying edge nodes close to data sources can complete data cleaning, feature extraction and fast inference locally, thereby reducing communication pressure and improving system real-time performance.

However, according to the existing research situation, the field of soil and water loss monitoring is still dominated by offline analysis, stage assessment and cloud centralized computing, and the integrated research on continuous perception, edge collaborative processing and trent-level dynamic prediction in complex field environment is still insufficient [7]. When multi-source sensor data continue to flood in, the traditional centralized architecture is easily restricted by transmission bandwidth, processing delay and node stability, and the local burst erosion process is difficult to capture in time, and the adaptation ability of the prediction results to the change of field conditions needs to be enhanced [8].

Based on the above problems, this paper studies the real-time monitoring and dynamic prediction system of soil and water loss supported by edge computing, and constructs a collaborative architecture of "perception layer-edge layer-cloud platform layer". At the system level, monitoring units such as rainfall, soil moisture, slope runoff, surface deposition change and vegetation state are set up to continuously collect and transmit erosion related information.

At the computing level, the edge nodes complete data preprocessing, local feature fusion and preliminary risk discrimination to reduce the load of the cloud. At the model level, a dynamic prediction method oriented to the collaboration of time evolution and spatial factors is introduced to realize the rapid identification of soil and water loss risk level and change trend. This study can provide realizable technical support for intelligent water conservation, mountain disaster early warning and fine decision-making of ecological governance.

# 2 Design of soil erosion real-time monitoring system

## 2.1 Overall architecture design of the system

In order to adapt to the application scenarios of discrete distribution of soil erosion monitoring objects, frequent environmental disturbances, diverse data sources and high warning response requirements, this paper designs the system as a hierarchical collaborative architecture supported by edge computing, and integrates real-time acquisition, edge processing, cloud analysis and early warning feedback into a unified link. The system design follows the four principles of stability, real-time, scalability and economy [9, 10]. The stability is mainly reflected in the redundant configuration of monitoring terminals, edge nodes and communication links. Even if local equipment fails, the system can still maintain key data acquisition and risk reporting functions. The real-time performance is reflected in the data preprocessing and preliminary discrimination moved to the edge side, so as to shorten the response path from the field perception to the risk output. The scalability is reflected in the modular interface design, which facilitates the subsequent access to new erosion factors, sensing devices and prediction algorithms. Economy runs through the whole process of hardware selection, node deployment and software architecture design, so as to control construction and operation and maintenance costs on the premise of ensuring performance [11, 12].

From the perspective of business requirements, the system needs to complete functions such as monitoring data collection, edge analysis, cloud storage, dynamic prediction, visual display and hierarchical early warning [13]. The collection end focused on the continuous perception of key indicators such as rainfall intensity, soil moisture content, slope change, runoff state, vegetation cover and surface sediment change. The edge side is responsible for outlier elimination, time series slicing, local feature extraction and risk initial screening. The cloud platform performs unified aggregation, model training, trend prediction and region-level risk interpretation on multi-point data. At the application level, the monitoring curve, spatial distribution and evolution process are displayed through a graphical interface, and an early warning is triggered when the threshold is exceeded or the trend is abnormal. The overall system architecture is shown in Figure 1.

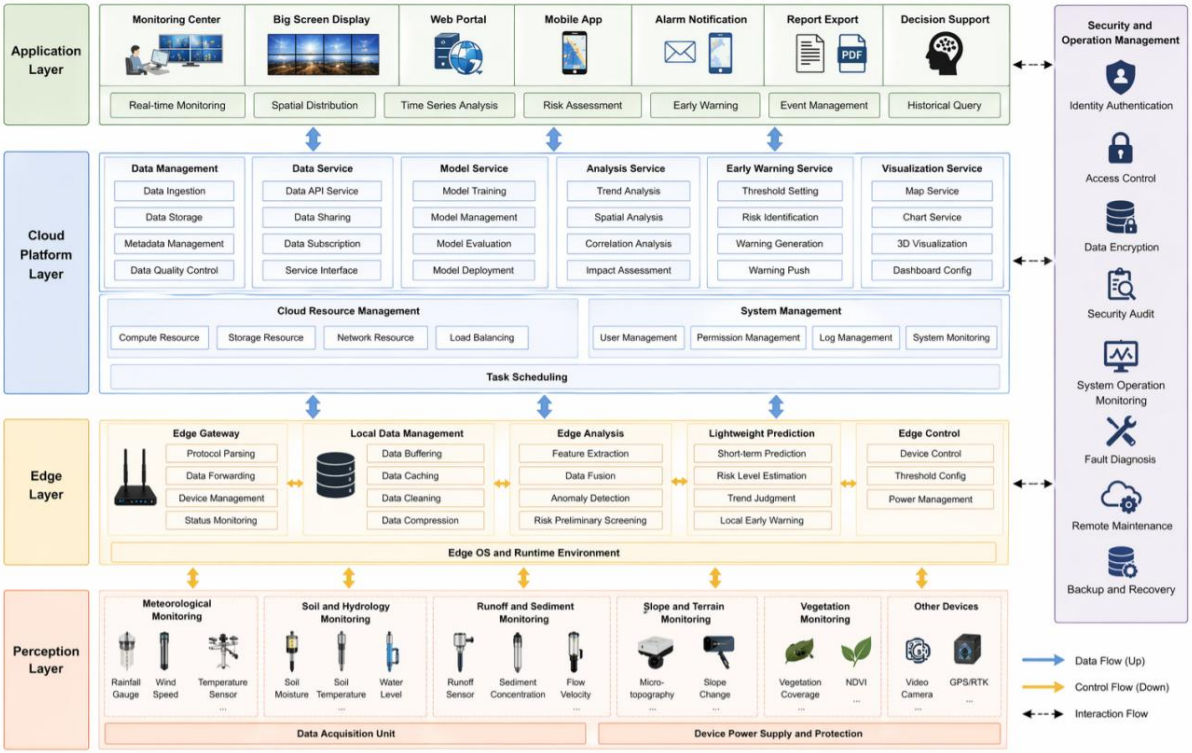


*Figure 1: Overall architecture of soil erosion real-time monitoring system*

In terms of structure division, this paper adopts a three-level architecture of "perception layer-edge layer-cloud platform layer". The perception layer was located at the front end of the field monitoring, which was responsible for the real-time acquisition of environmental information and signal digitization. The edge layer is deployed near the monitoring site and undertakes the tasks of data cleaning, compression, fusion and local inference. The cloud platform layer is responsible for cross-regional data aggregation, historical sample management, model iterative update and large-screen display. Each layer has a clear division of labor and is connected with each other, which can form a closed-loop operation mechanism from field perception to decision feedback. Table 1 shows the main functional modules and corresponding tasks of the system.

*Table 1: System functional modules and main tasks*

| Module Level | Core Module | Main Task |
|---|---|---|
| Perception layer | Multi-source sensing unit | Collects rainfall, moisture, runoff, sediment, slope morphology, and vegetation information |
| Edge layer | Edge gateway and local analysis module | Performs data cleaning, feature extraction, local fusion, anomaly identification, and preliminary prediction |
| Cloud platform layer | Data center and model service | Supports historical storage, global training, trend analysis, and model updating |
| Application layer | Visualization and early warning module | Provides risk display, threshold warning, report output, and decision support |

## 2.2 System hardware design

The hardware design of the system is centered on the requirements of "field deployment,

continuous operation, and adaptability to complex environments". The sensing unit adopts a modular configuration to improve the comprehensive characterization ability of the erosion process [14]. The rainfall acquisition module uses a bucket rainfall sensor to record the start and end time of rainfall events, cumulative rainfall and short-term rain intensity. The soil moisture module uses a capacitive sensor to reflect the change of soil water state. The slope runoff monitoring module obtains the surface confluence characteristics through the flow velocity and flow integration device. The sediment monitoring module combined with turbidity or suspended particle detection devices to estimate the migration intensity of erosion materials. In scenarios where micro-deformation of slope needs to be identified, dip Angle or micro-terrain acquisition devices can be added to assist in judging the slope instability trend [15, 16]. Considering the unstable power supply of the field monitoring point, the terminal node adopts the combination of solar power supply and battery energy storage to ensure long cycle operation.

The data acquisition and edge processing part is based on a low-power embedded controller and an industrial-grade edge gateway. The former is responsible for multi-channel sensing interface access, analog-to-digital conversion, timing sampling and local cache, while the latter is responsible for protocol conversion, task scheduling and lightweight model inference [17]. In order to adapt to the communication differences in mountainous areas, slope areas and small watershed environments, the system supports multiple communication methods such as LoRa, 4G/5G and Ethernet, which can be flexibly deployed according to site conditions. The hardware configuration is shown in Table 2.

*Table 2: Main hardware components and functions of the system*

| Hardware Type | Typical Device | Main Function |
|---|---|---|
| Rainfall monitoring unit | Tipping-bucket rain gauge | Acquires cumulative rainfall and short-term rainfall intensity |
| Soil monitoring unit | Capacitive moisture sensor | Reflects changes in soil moisture content |
| Runoff monitoring unit | Flow velocity/flow rate acquisition device | Monitors slope-surface or channel runoff conditions |
| Sediment monitoring unit | Turbidity/particle concentration sensor | Characterizes the transport intensity of eroded materials |
| Edge device | Industrial gateway, embedded controller | Performs local computation, buffering, and protocol conversion |
| Power supply and communication | Solar modules, storage battery, LoRa/4G/wired backhaul | Supports long-term operation and remote transmission |

## 2.3 System software design

The software system was implemented by combining front-end and back-end separation and cloud-edge collaboration. The acquisition program of the perception layer runs in the embedded environment, adopts the modular driver architecture to manage various sensors, and completes initialization, sampling control, data verification and cache writing [18]. In order to deal with the problem of unstable network in the wild, the program built-in breakpoint continuation and local cache mechanism, when the communication is interrupted, the data is temporarily stored, and the data is uploaded in batch after the link is restored, thereby reducing the loss of observation sequence.

The edge-layer communication and processing program is responsible for implementing

multi-protocol access, message scheduling, and local analysis. The communication layer used MQTT combined with TCP/IP to complete lightweight publish/subscribe and stable network transmission. The processing layer organizes continuous samples through the sliding window mechanism, carries out denoising, normalization, outlier identification and feature construction on the original data, and encodes information such as short-term rainfall fluctuation, humidity accumulation effect, runoff mutation and sediment response into input vectors that can be used for dynamic prediction [19, 20]. For the problem of limited computing resources of edge devices, the system deployed the model as a compressed lightweight version, and only output the risk level and early warning signs at the edge side, while complex training and global calibration were still performed in the cloud.

The application layer software mainly completes data management, result display and early warning services. The back-end of the platform adopts the architecture of separating database and model service, which supports monitoring record storage, historical query, model version management and log tracking. The front end displays monitoring curves, site maps, risk hot spots and trend comparison results with visual components, which facilitates managers to grasp the erosion evolution process [21]. The warning module supports dual mechanisms of threshold warning and trend warning. When the current index exceeds the set range, the system immediately triggers an alarm. Even if the boundary has not been crossed, as long as the model judges that there is a significant upward trend in a short period of time, it will push the risk warning in advance. The software operation logic is shown in Figure 2.

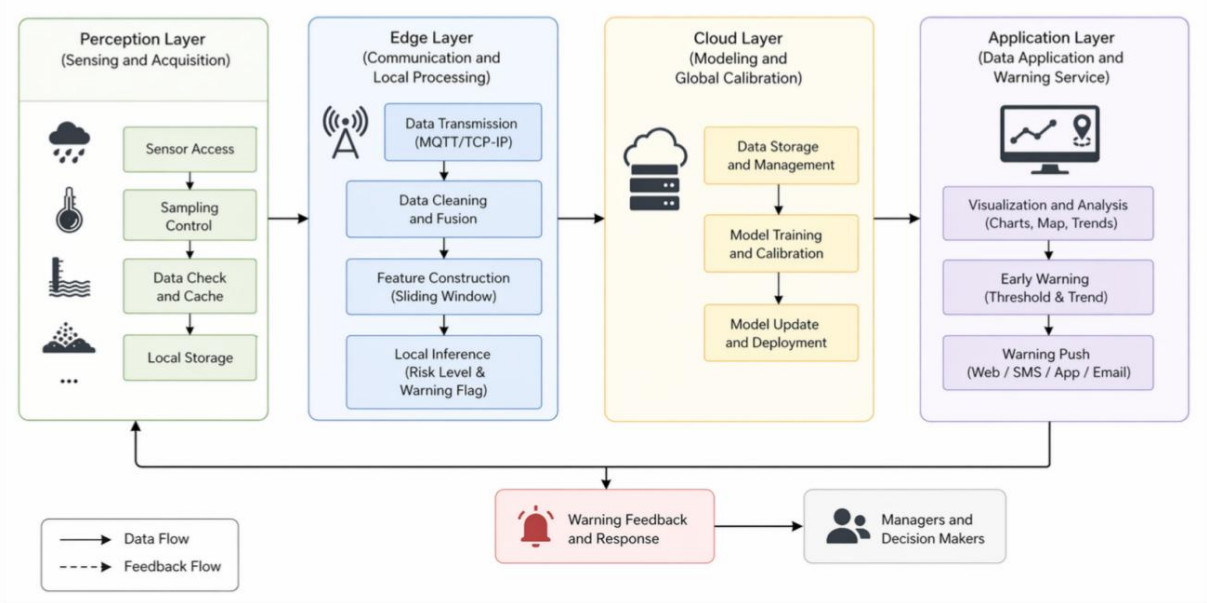


*Figure 2: Flow chart of system software operation and early warning feedback*

Through the above software and hardware co-design, the system can change the data processing link from "centralized upload and unified calculation" to a distributed mode of "on-site perception, edge initial judgment, and cloud collaboration" on the basis of ensuring continuous on-site collection, so as to provide a stable, timely, and spatially specific input basis for the construction of subsequent dynamic prediction models of soil erosion.

# 3 Design of soil and water loss dynamic prediction model based on edge computing collaboration

## 3.1 Limitations of traditional soil and water loss monitoring and prediction methods

Traditional soil and water loss monitoring and forecasting methods have a certain application basis in regional investigation, erosion classification and risk identification. However, when the monitoring goal turns to continuous perception, rapid response and dynamic prediction, the shortcomings of the method structure gradually appear. Existing studies mostly rely on manual inspection, remote sensing periodic interpretation, empirical statistical models, hydrological process models, and cloud-based centralized computing frameworks. These methods can describe the medium-and long-term erosion distribution patterns, but they are difficult to adapt to the monitoring scenarios of short-term heavy rainfall, sudden changes in slope runoff and rapid development of local erosion. Especially in the complex slope environment, rainfall, soil moisture, vegetation cover, slope morphology and sediment migration are not linearly synchronized. If static parameters or fixed weight structures are still used to process multi-source data, it is easy to weaken the representation ability of key disturbance information. Taking the traditional weighted fusion method as an example, the erosion risk at a certain time is often expressed as follows.

$$R_t = \sum_{i=1}^{m} \alpha_i \, x_{i,t} \tag{1}$$

Here, $x_{i,t}$ denote the type i monitoring factor at time t, $\alpha_i$ is the preset weight, and m is the number of factors. These methods are simple in form, but the weights are usually fixed in the modeling stage, which is difficult to adaptively adjust with the advance of rainfall process, the change of soil saturation degree and the enhancement of slope response. When local monitoring points have abnormal fluctuations in a short period of time, the fixed-weight model often cannot amplify the high-risk signal in time, which leads to the erosion trend identification lag.

On the other hand, although the traditional time series model has certain advantages in continuous series processing, it still has obvious limitations when facing multi-source heterogeneous data of soil and water loss. The rainfall sequence is abrupt, the humidity evolution is cumulative, and the runoff and sediment changes are phased and spatially dependent. The sampling frequency, dimension range and response rhythm are not consistent between different data. If only a single time recurrence structure is used to process all the inputs, the model is easier to learn the average change trend, but it is not sensitive enough to the local anomaly before burst erosion. The traditional centralized processing mode also introduces additional delay, and its total response time can be expressed as:

$$T_{all} = T_{up} + T_{queue} + T_{cloud} + T_{return} \tag{2}$$

where $T_{up}$ is the data upload time, $T_{queue}$ is the queuing waiting time, $T_{cloud}$ is the cloud computing time, and $T_{return}$ is the result return time. When the number of monitoring points increases, images and sensor data are uploaded concurrently, or the network link is unstable, $T_{all}$ will increase significantly, which will affect the real-time warning effect.

In addition, the traditional methods generally have the problem of insufficient utilization of spatial correlation. Soil erosion is not a single point isolated event, but a dynamic evolution

process formed by the joint action of slope position difference, land cover, confluence path and peripheral disturbance. If the model is judged only from the historical sequence of a single monitoring point, but lacks the joint expression of adjacent slope units, upstream and downstream transmission relationships and regional terrain constraints, it is difficult to accurately reveal the erosion expansion direction and risk propagation path. Figure 3 shows the main shortcomings of traditional monitoring and prediction methods in terms of multi-source data access, spatio-temporal correlation expression, and real-time response. It can be seen that for the real-time monitoring task of soil and water loss, only relying on the traditional centralized analysis and static prediction framework is difficult to meet the actual needs of parallel promotion of high-frequency sampling, edge response and dynamic analysis, which also provides a clear problem direction for the subsequent introduction of edge computing collaborative mechanism.

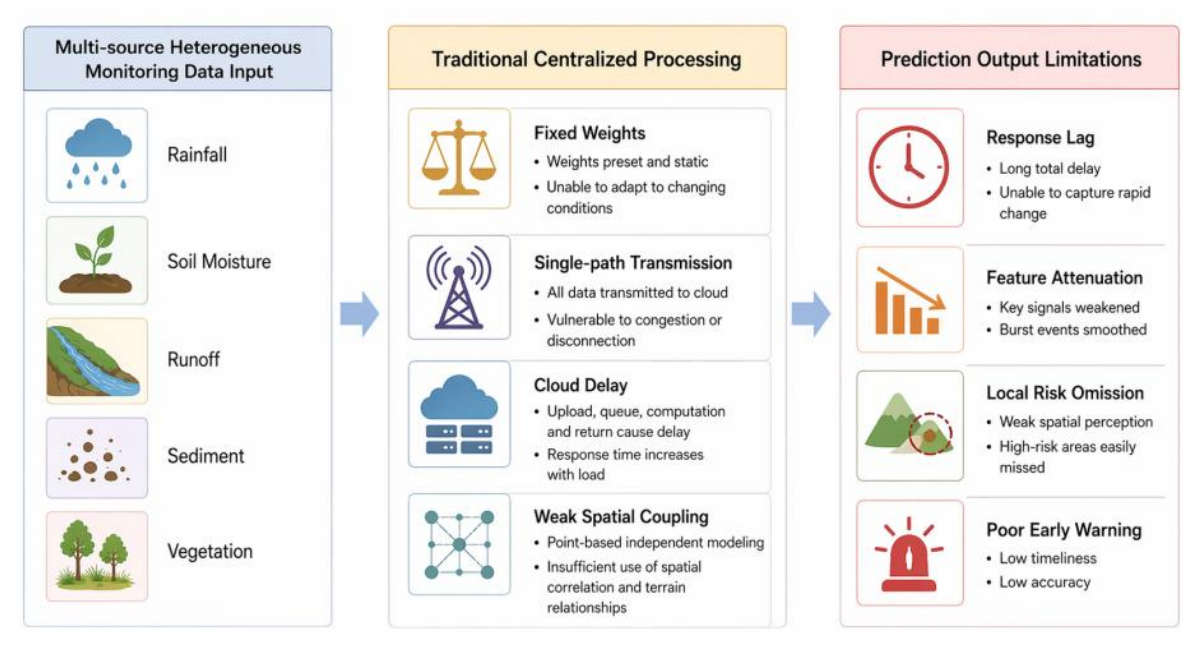


*Figure 3: Schematic diagram of the limitations of traditional soil and water loss monitoring and prediction methods*

## 3.2 Principle of dynamic prediction method supported by edge computing

In the real-time monitoring scenario of soil and water loss, the dynamic prediction is not a simple extrapolation of the monitoring value at a single time point, but a computational expression of the continuous coupling relationship between rainfall disturbance, soil moisture state, slope confluence process, land cover change and erosion response. Since the monitoring terminals are distributed in different slope positions, channels and surface units, the data not only have the characteristics of abrupt change and lag in time, but also have the spatial correlation and transfer effect. If the processing method is still single path and single scale, the model is difficult to make fine-grained identification of the erosion evolution process. Based on this, this paper combines the near-source computing power of edge nodes with the dynamic prediction model, completes the short-term sequence organization, local feature screening and preliminary fusion at the edge, and completes the global parameter update and model correction in the cloud, thus forming a dynamic prediction method for real-time

monitoring tasks. The basic principle is shown in Figure 4.

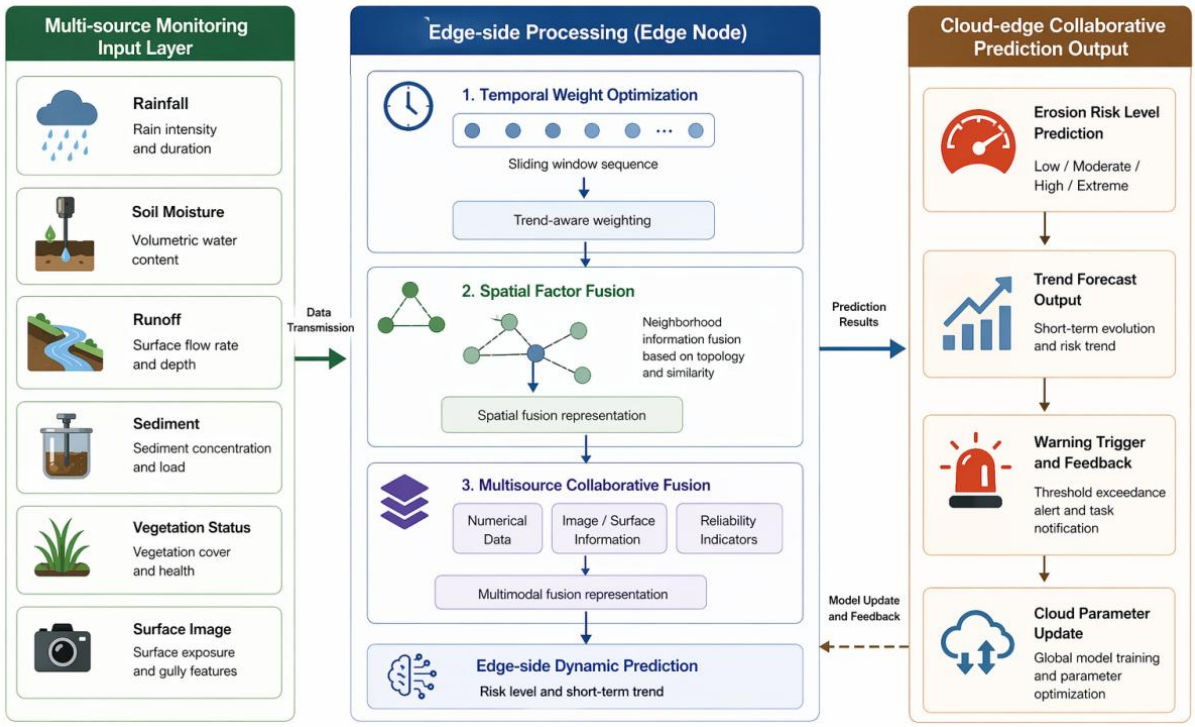


*Figure 4: Schematic diagram of the dynamic soil and water loss prediction method supported by edge computing*

### 3.2.1 Time dimension Feature Modeling and Weight Optimization

The process of soil erosion is obviously event-driven. A short duration heavy rainfall may lead to enhanced surface runoff, rapid rise of soil moisture content and abrupt change of sediment transport in a very short time. After the rainfall, the slope response will show a phased change of attenuation and lag. Therefore, the key to modeling the temporal dimension is not only to memorize the historical data, but also to identify the mutation fragments, continuous accumulation and turning points in the monitoring sequence. Let the input feature vector received by an edge node at time t be $x_t \in \mathbb{R}^d$, and the local sequence consisting of the last L moments be denoted as follows.

$$H_t = [x_{t-L+1}, x_{t-L+2}, \cdots, x_t] \tag{3}$$

Here, d is the feature dimension at a single moment, and L is the edge side sliding window length. Traditional time series attention usually assigns weights only based on feature similarity, which is difficult to reflect the trend information carried by rainfall spikes, runoff turns or sediment spikes. In order to enhance the sensitivity of the model to changes in erosion precursors, this paper introduces a time trend factor $\eta_t$ on the edge side and modifies the original attention score. The weighting coefficient of time τ on the current time t is defined as:

$$\alpha_{\tau,t} = \frac{\exp(s_{\tau,t} + \lambda\eta_\tau)}{\sum_{j=t-L+1}^{t} \exp(s_{j,t} + \lambda\eta_j)} \tag{4}$$

Here, $s_{\tau,t}$ is the base similarity score and λ is the trend adjustment coefficient. This

equation shows that the time weight is no longer determined by the similarity only, but is affected by the change trend at the same time. When there is an abnormal rise or rapid fluctuation in a certain period, its contribution in the sequence representation is actively amplified.

The trend factor $\eta_\tau$ is determined by both the rate of change at adjacent moments and the local statistics. Let the comprehensive change rate of the key erosion index be $\Delta_t$, then:

$$\Delta_t = \frac{\|x_t - x_{t-1}\|_2}{\|x_{t-1}\|_2 + \varepsilon} \tag{5}$$

$$\eta_t = \sigma\left(\frac{\Delta_t - \mu_\Delta}{\sigma_\Delta + \varepsilon}\right) \tag{6}$$

where $\mu_\Delta$ and $\sigma_\Delta$ represent the mean and standard deviation of the rate of change in the current window, $\sigma(\cdot)$ is the Sigmoid function, and $\varepsilon$ is a small constant to prevent the denominator from being zero. When the change rate is significantly higher than the local average level at a certain time, $\eta_t$ is close to 1, and the model will increase the time series weight of the corresponding segment. When the sequence changes more gently, $\eta_t$ decreases accordingly, and the model pays more attention to the continuous cumulative features rather than short-time noise. This processing method is suitable for the sequence structure of "emergency trigger-continuous response evolution" in soil and water loss monitoring tasks, and also facilitates edge devices to quickly locate high-risk segments with limited computing resources. On this basis, the temporal aggregation features output by the edge nodes can be expressed as follows.

$$z_t^{(T)} = \sum_{\tau=t-L+1}^{t} \alpha_{\tau,t}\, x_\tau \tag{7}$$

This feature not only retains local historical information, but also highlights the abnormal change period through the trend enhancement mechanism, which provides a more stable time representation for subsequent spatial fusion and multi-source collaboration.

### 3.2.2 Spatial dimension erosion factor fusion strategy

Different from the general equipment condition prediction, the monitoring objects of soil and water loss are not located inside the closed system, but are distributed in the open space with topographic differences and confluence relations. After rainfall action on different slope positions, the erosion response tends to expand gradually along slope aspect, channel and underlying surface conditions. The risk of local monitoring sites is not completely determined by their own sequence, but is also closely related to the change of runoff production, sediment transport and cover state of adjacent units. If the model only uses a single point of data to judge, it is easy to ignore the spatial transmission path and regional coupling relationship. Based on this, this paper constructs a spatial erosion factor fusion strategy supported by edge computing, organizes the information of multiple monitoring points into local spatial subgraphs, and completes the neighborhood feature weighting on the edge side.

Let the temporal aggregation characteristic of site i at time t be $z_{i,t}^{(T)}$ and its neighborhood set be $\mathcal{N}(i)$. The spatial influence weight of site j on site i is defined as by combining topographic proximity, confluence direction and transmission accessibility:

$$\omega_{ij,t} = \frac{\exp\left(\rho\, a_{ij} + \kappa\, \cos\left(z_{i,t}^{(T)}, z_{j,t}^{(T)}\right)\right)}{\sum_{m\in\mathcal{N}(i)} \exp\left(\rho\, a_{im} + \kappa\, \cos\left(z_{i,t}^{(T)}, z_{m,t}^{(T)}\right)\right)} \tag{8}$$

Here, $a_{ij}$ represents the static spatial correlation strength composed of slop location connectivity, aspect consistency or runoff path relationship, $\cos(\cdot,\cdot)$ represents the characteristic cosine similarity, and $\rho$ and $\kappa$ are the adjustment parameters. This formula takes into account both spatial structure prior and real-time state similarity: if two monitoring points are closer in terrain connection and show similar erosion response characteristics at the current time, their interaction weight will be increased. On the contrary, if two points are adjacent in space, but the state change difference is large, the association will be suppressed. Accordingly, the spatial fusion feature of site i can be written as follows.

$$z_{i,t}^{(S)} = \sum\nolimits_{j\in\mathcal{N}(i)} \omega_{ij,t}\, W_s z_{j,t}^{(T)} \tag{9}$$

Here, $W_s$ is the spatial mapping matrix. The role of this mechanism is not to simply average neighborhood information, but to automatically strengthen the influence of key slope segments, key channels, or upstream nodes on the current site according to the spatial transfer logic of the erosion process. The spatial fusion module can introduce the upstream anomaly information into the current representation in advance to improve the ability to judge the erosion expansion trend when the monitoring point on the surface of a slope has enhanced rainfall and runoff surge, but the lower station has not responded significantly. Compared with the traditional static superposition method, this strategy is more suitable for describing the process characteristics of soil and water loss from local disturbance to regional diffusion.

### 3.2.3 Collaborative fusion mechanism of multi-source monitoring data

Real-time monitoring of soil and water loss involves rainfall, humidity, runoff, sediment, vegetation, microtopography and some image recognition results. Different modalities have obvious differences in sampling frequency, dimensional unit, noise level and information expression. Numerical data can reflect continuous physical changes, while images or land surface state recognition results are more suitable for revealing morphological information such as slope bare surface, gully erosion boundary and cover degradation. If all kinds of data are directly concatenated into the model, it is not only easy to introduce dimensional bias, but also may amplify the interference of low-quality data on the results. In order to improve the collaborative fusion effect, this paper sets up a multi-source data consistency processing and reliability correction mechanism at the edge side, and completes the global fusion parameter optimization in the cloud.

Let the numerical monitoring vector be $u_t$, the image parsing or land surface state coding result be $g_t$, and the node communication quality, sensing health and data integrity together constitute the reliability vector rt. After standardization and mapping, the multi-source fusion representation is defined as follows.

$$f_t = \phi\left(W_u u_t + W_g g_t + W_r r_t + b\right) \tag{10}$$

where $W_u, W_g, W_r$ are the mapping parameters of different data channels, b is the bias term, and $\phi(\cdot)$ is the nonlinear activation function. The purpose of introducing the reliability vector is to make the model distinguish between "data mutation caused by environment anomaly"

and "data anomaly caused by equipment drift or link fluctuation". When a sensor drops the line for a short time, the sampling is unstable, or the noise is enhanced, the fusion module will automatically downregulate its influence on the final representation, so as to improve the operation robustness of the system in the complex environment.

Furthermore, in order to realize the collaboration between real-time reasoning on the edge side and global calibration on the cloud, the temporal feature $z_t^{(T)}$, spatial feature $z_t^{(S)}$ and multi-source fusion feature $f_t$ are jointly constructed as the dynamic prediction input:

$$h_t = W_h [z_t^{(T)} \parallel z_t^{(S)} \parallel f_t] + b_h \tag{11}$$

Here, $\parallel$ denotes the feature concatenation, $W_h$ and $b_h$ are the parameters of the fusion layer. The edge node outputs the current risk level and short-term trend judgment based on ht, and the cloud receives the edge summary data and key samples periodically, updates the parameters, and then synchronizes them to each edge node. In this way, the system not only retains the advantage of low delay of edge inference, but also avoids the decline of adaptability caused by long-term fixed model.

## 3.3 Dynamic prediction model construction and training

### 3.3.1 Model structure design

After the time dimension weight optimization, the spatial dimension erosion factor fusion and the collaborative representation of multi-source monitoring data, it is necessary to further build a trainable and deployable dynamic prediction model to support the rapid inference of edge nodes and the global correction of cloud platform. Considering that soil and water loss monitoring data have the characteristics of short-term mutation, stage continuation, spatial transmission and modal heterogeneity, this paper adopts the overall structure of "spatio-temporal attention feature extraction-convolutional sequence encoder-gated temporal modeling-dual task output". The input layer receives the fusion feature sequence uploaded by the edge side, and maps the coding results of rainfall, soil moisture, runoff, sediment, vegetation state and land surface morphology into the same expression space. After the processing of the aforementioned time and space modules, the spatio-temporal fusion representation $h_t$ is obtained, and a sliding window of length L is used to construct continuous input segments:

$$X_t = [h_{t-L+1}, h_{t-L+2}, \cdots, h_t] \tag{12}$$

This representation not only preserves the mutation information in the local event process, but also maintains the continuous evolution characteristics of the erosion response over a period of time. In order to extract the local fluctuation pattern on a short time scale, this paper introduces a one-dimensional convolution structure in the feature extraction layer to perform convolution mapping on the combination of changes at adjacent moments in the window, and its output is defined as:

$$c_t = \phi(W_c * X_t + b_c) \tag{13}$$

where $W_c$ is the convolution kernel parameter, $b_c$ is the bias term, and $\phi(\cdot)$ is the activation function. The role of the convolutional layer is to capture short-time coupling patterns such as heavy rainfall trigger, moisture accumulation, runoff enhancement and sediment surge rise, so as to improve the recognition ability of the model for erosion precursor signals.

After the convolution output, this paper uses a gated recurrent unit to further model the time dependence. Different from relying solely on convolution to extract local patterns, the gated recurrent structure is more suitable for expressing the lag effect and continuous accumulation characteristics in the process of slope erosion. Its hidden state update can be expressed as follows.

$$s_t = (1 - z_t) \odot s_{t-1} + z_t \odot \tilde{s}_t \tag{14}$$

Here, $z_t$ is an update gate, $\tilde{s}_t$ is a candidate state, and $\odot$ represents element-wise multiplication. This structure can not only maintain important historical information, but also avoid excessive interference caused by redundant fluctuations on sequence expression, making the model more suitable for dealing with complex time-varying relationships in continuous monitoring environments.

The output layer adopts a double-branch design. One branch is used to distinguish the erosion risk level and output the probability distribution of discrete categories such as low, medium and high. The other branch is used for continuous prediction of erosion intensity or risk index to reflect the change trend in the future for a short period of time. The risk classification branch uses the Softmax function, whose output is:

$$p_t^{(k)} = \frac{\exp\left(o_t^{(k)}\right)}{\sum_{j=1}^{K} \exp\left(o_t^{(j)}\right)} \tag{15}$$

Here, $o_t^{(k)}$ represents the discrimination score of the KTH risk state at time t, and k is the total number of risk categories. Through the above structure, the model can not only complete real-time risk identification, but also provide continuous trend basis for subsequent early warning modules. The overall structure is shown in Figure 5.

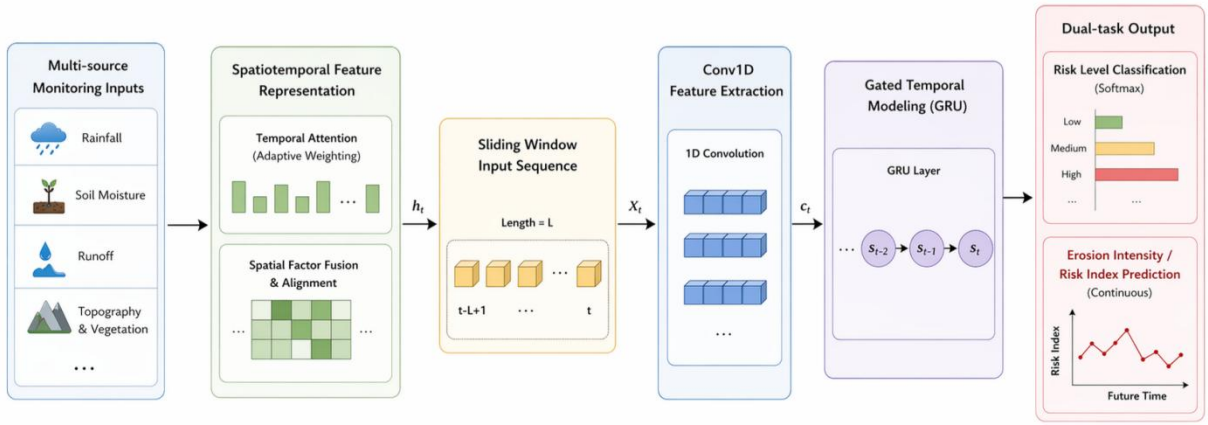


*Figure 5: Schematic diagram of the dynamic prediction model structure*

### 3.3.2 Training dataset processing

In order to ensure that the model training process is consistent with the actual monitoring scene, this paper constructs the training data set as a joint data form of "on-site continuous monitoring samples + simulation supplementary samples". The field data mainly come from the continuous sampling records of typical slopes, channel nodes and small watershed monitoring stations, and the simulation data are used to supplement the problem of insufficient samples under extreme rainfall and high erosion stages. The two types of data are

unified for time alignment, dimension correction, missing completion and label mapping before storage to avoid the structural deviation of data from different sources.

Since multi-source monitoring data are affected by equipment drift, communication anomaly and environmental disturbance, there are often outliers and local noise in the original samples. To this end, this paper firstly eliminates obvious abnormal segments according to the sensing state log and statistical threshold rules, and then performs window segmentation on continuous sequences to construct supervised samples for dynamic prediction. For any original sequence $Q = \{q_1, q_2, \cdots, q_T\}$, the training samples are generated by sliding with step size r, so that each sample contains both historical observation segments and future prediction labels. This processing method is conducive to improving the learning ability of the model for continuous event chains, rather than making static judgments only based on isolated moments. In the normalization stage, the min-max mapping method is used to uniformly scale the features of different dimensions:

$$x' = \frac{x - x_{min}}{x_{max} - x_{min}} \tag{16}$$

This method can compress different dimensional data such as rainfall, humidity value, runoff intensity and sediment concentration into the same numerical interval, and weaken the influence of scale differences on training stability. Then, all the samples were divided into training set, validation set and test set according to the ratio of 7:2:1. The training set is used to learn the model parameters, the validation set is used to adjust the hyperparameters such as the number of convolution kernels, hidden layer dimensions, learning rate and window length, and the test set is used to evaluate the generalization ability of the model on unseen samples.

Considering the low proportion of high-risk erosion samples in the natural monitoring data, if the ordinary loss function is directly used, the model is easy to be biased to the dominant distribution in the middle and low risk stage of learning, thus weakening the ability to identify sudden erosion events. Based on this, this paper adopts the training strategy of joint optimization of classification loss and regression loss to unify the risk level recognition and trend prediction into the same objective function:

$$\mathcal{L} = \lambda_1 \mathcal{L}_{cls} + \lambda_2 \mathcal{L}_{reg} \tag{17}$$

Here, $\mathcal{L}_{cls}$ is used to constrain the risk classification result, $\mathcal{L}_{reg}$ is used to constrain the continuous prediction error, and $\lambda_1$ and $\lambda_2$ are the balance coefficients of the two-part loss. The joint training method can make the model maintain the sensitivity to the change of erosion intensity while learning the category boundaries, which is more in line with the requirements of "discrimination + trend" dual output of real-time early warning tasks.

In the training process, the parameter update is completed in the cloud, and the compressed model is synchronized to the edge node regularly. At the edge side, only the lightweight parameters required for inference are retained to ensure that the field equipment can complete the fast prediction with limited computing power. The cloud is responsible for model iteration, error propagation, and version management. Through this training and deployment mechanism, the model not only has good global learning ability, but also can meet the operation requirements of real-time monitoring system for low delay and strong adaptability.

# 4 Experimental simulation and result analysis

## 4.1 Construction of experimental environment

In order to test the feasibility of the system in continuous monitoring, edge reasoning and dynamic prediction, this paper builds an experimental environment composed of front-end sensor nodes, edge gateways, wireless transmission links and cloud analysis platforms, and carries out joint tests in typical slope monitoring scenarios and simulation supplementary scenarios. The hardware platform is based on the collaboration of multi-source acquisition and near-source calculation, and it is equipped with rainfall, soil moisture, slope runoff, sediment concentration and inclination sensing units at the monitoring end. Among them, the resolution of the rainfall sensor is 0.2 mm, the measurement range of soil moisture is 0 ~ 100%, and the accuracy is ±2.0%. The sampling interval of the runoff flow module is set to 1 min, and the range of the sediment concentration detection module is 0 ~ 20 g/L. The edge node uses a four-core industrial gateway with a main frequency of 1.8 GHz, 4 GB memory and 64 GB local cache capacity, which can complete data cleaning, sliding window segmentation and lightweight model reasoning on the site side. The cloud server is equipped with Intel Xeon Silver 4310 CPU, 64 GB memory and NVIDIA RTX 4080 16 GB graphics card for model training, parameter update and visual analysis.

The software environment uses Ubuntu 22.04 operating system, Python 3.11 and lightweight inference framework are deployed on the edge side, and PyTorch 2.2, NumPy, Pandas and Matplotlib are used in the cloud training platform to complete data processing, model training and result analysis. The communication layer also supports transmission modes such as LoRa, 4G and wired backtransmission. Under normal link conditions, the data upload delay from edge nodes to the cloud is kept at a low level, and the average upload delay is 84 ms under 4G conditions, which can still maintain a stable data arrival rate in continuous concurrent upload scenarios. In order to ensure that the experimental process is consistent with the actual business, the system first aggregates the front-end sampling data at the edge end for 10 minutes, and then uploads the key features and early warning results synchronously, so as to reduce the bandwidth pressure caused by the full transmission of the original sequence for a long time.

The experimental data set consists of measured samples and simulation samples. In the measured part, the continuous observation data of 12 monitoring points in a typical small watershed in northern Shaanxi from May 2023 to October 2024 were selected, and 286,400 valid time series records were accumulated. In the simulation part, 41,600 samples were added for short-duration rainstorm, continuous rainfall, and enhanced vegetation disturbance, which were used to enhance the training coverage of the high-risk stage. After outlier elimination, missing imputation and normalization, a total of 328,000 available records were obtained, which were divided into training set, validation set and test set according to 7:2:1. The risk labels are jointly calibrated according to runoff intensity, sediment concentration growth rate and slope response grade, and are divided into three categories: low risk, medium risk and high risk. The experimental environment and data configuration are shown in Table 3.

*Table 3: Experimental environment and dataset configuration*

| Category | Configuration Content | Parameter or Scale |
|---|---|---|
| Monitoring terminal | Rainfall sensor | Resolution: 0.2 mm |
| Monitoring terminal | Soil moisture sensor | Range: 0–100%, accuracy: ±2.0% |
| Monitoring terminal | Runoff/sediment monitoring module | Sampling interval: 1 min, sediment range: 0–20 g/L |
| Edge device | Industrial gateway | 4-core 1.8 GHz, 4 GB RAM, 64 GB storage |
| Cloud platform | Training server | Xeon Silver 4310, 64 GB RAM, RTX 4080 16 GB |
| Software environment | Operating system and development environment | Ubuntu 22.04, Python 3.11, PyTorch 2.2 |
| Data scale | Measured samples | 286,400 records |
| Data scale | Simulated supplementary samples | 41,600 records |
| Data split | Training/validation/test | 229,600 / 65,600 / 32,800 |

## 4.2 System performance test

In order to test the operation ability of the system designed in this paper under complex monitoring scenarios, this paper comprehensively tests the accuracy of data acquisition, the stability of network transmission, the efficiency of system response and the reliability of continuous operation based on the experimental environment in Section 4.1. The main results are shown in Table 4. Test results show that the system can stably complete real-time access and fast feedback of multi-source monitoring data under the support of edge computing. In terms of acquisition accuracy, the results of standard rain gauge, portable soil moisture content meter and laboratory sediment concentration measurement were selected as controls to compare the continuous 48 h monitoring data. The mean absolute error of rainfall measurement was 0.41 mm, the relative error was 1.87%, and the mean absolute error of soil moisture measurement was 1.63%. The mean absolute error of sediment concentration measurement is 0.28 g/L, which indicates that the front-end perception module can accurately reflect the change of slope environment. In the network transmission test, the continuous upload process under three conditions of 4G, LoRa relay and wired backhaul was simulated respectively. After the edge side adopted the MQTT message mechanism and the local cache cooperation strategy, the average packet loss rate of 4G link was controlled at 1.6%, LoRa relay link was 2.4%, and wired backhaul was only 0.2%. The corresponding average delay is 84 ms, 132 ms and 19 ms respectively, which can meet the requirements of real-time monitoring system for short-period data reporting.

*Table 4: System performance test results*

| Test Item | Indicator | Test Result |
|---|---|---|
| Data acquisition accuracy | Mean absolute error of rainfall | 0.41 mm |
| Data acquisition accuracy | Mean relative error of rainfall | 1.87% |
| Data acquisition accuracy | Mean absolute error of soil moisture | 1.63% |
| Data acquisition accuracy | Mean absolute error of sediment concentration | 0.28 g/L |
| Network transmission stability | Average packet loss rate of 4G | 1.6% |
| Network transmission stability | Average packet loss rate of LoRa relay | 2.4% |
| Network transmission stability | Average packet loss rate of wired backhaul | 0.2% |
| Network transmission stability | Average latency of 4G/LoRa/wired transmission | 84/132/19 ms |
| System response efficiency | Average response time | 1.12 s |
| System response efficiency | Reduction ratio compared with centralized architecture | 31.4% |
| Long-term operational reliability | Continuous operating duration | 72 h |
| Long-term operational reliability | Average CPU/memory utilization | 38.6% / 43.1% |

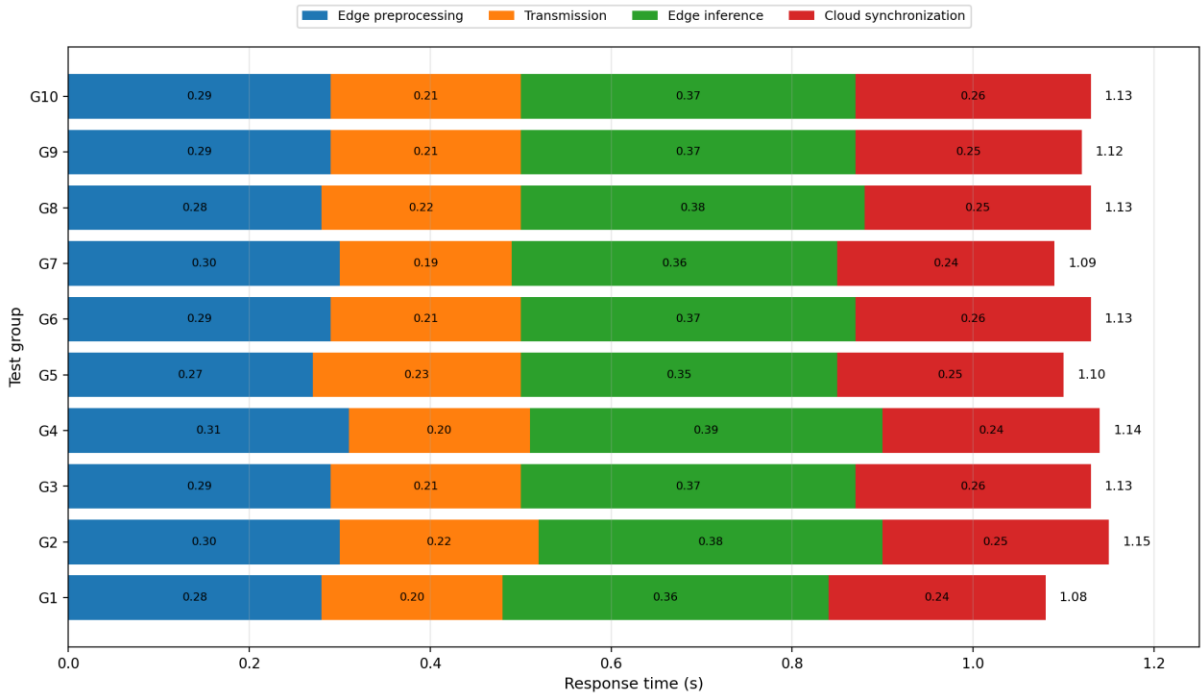


*Figure 6: Composition and distribution of system response time*

In the system response time test, this paper constructed three typical scenarios: short-term heavy rainfall trigger, rapid rise of slope humidity and sudden increase of sediment concentration, and recorded the whole process time consumption from sensing sampling to application layer early warning output. The composition and distribution results of response time are shown in Figure 6. The results of 100 repeated tests show that the average response time of the system is 1.12 s, of which the edge side data cleaning and feature construction

takes about 0.29 s, the network transmission takes an average of 0.21 s, the edge reasoning and early warning generation takes 0.37 s, and the cloud synchronization and interface refresh takes 0.25 s. Compared with the traditional centralized processing method, the average response time of the proposed system is reduced by 31.4%, indicating that the delay pressure caused by cloud queuing and full upload can be effectively reduced after preprocessing and preliminary discrimination are moved to the edge node. In order to further study the long-term operation stability, the system runs continuously for 72 h in a typical monitoring scenario, during which the average CPU occupancy rate of the edge gateway is 38.6%, and the memory occupancy rate is 43.1%. There are only two short-term link fluctuations, which return to normal after automatic reconnection, and there is no continuous data loss, abnormal program exit or device offline phenomenon.

## 4.3 Special test of algorithm performance

In order to further verify the applicability of the dynamic prediction model constructed in this paper in the real-time monitoring task of soil and water loss, LSTM, GRU and the spatio-temporal fusion model without introducing edge collaborative optimization are selected as the comparison objects, and special tests are carried out under the same training set, validation set and test set conditions. The test results show that the proposed model shows strong advantages in multiple indicators. As shown in Figure 7, the Accuracy, Recall and F1 of the proposed model on the test set reach 95.8%, 94.9% and 95.3%, respectively, which are significantly higher than 87.6%, 86.8% and 87.1% of LSTM. It is also better than 89.4%, 88.6% and 89.0% of GRU, and 5.7, 5.9 and 5.8 percentage points higher than the unimproved spatio-temporal fusion model, respectively. This shows that after the introduction of time weight optimization, spatial neighborhood fusion and multi-source collaboration mechanism, the recognition ability of the model for key erosion signals such as short-time heavy rainfall trigger, sudden increase of slope runoff and abnormal increase of sediment concentration has been enhanced, especially under the condition of low proportion of medium-high risk samples, it can still maintain good discrimination stability.

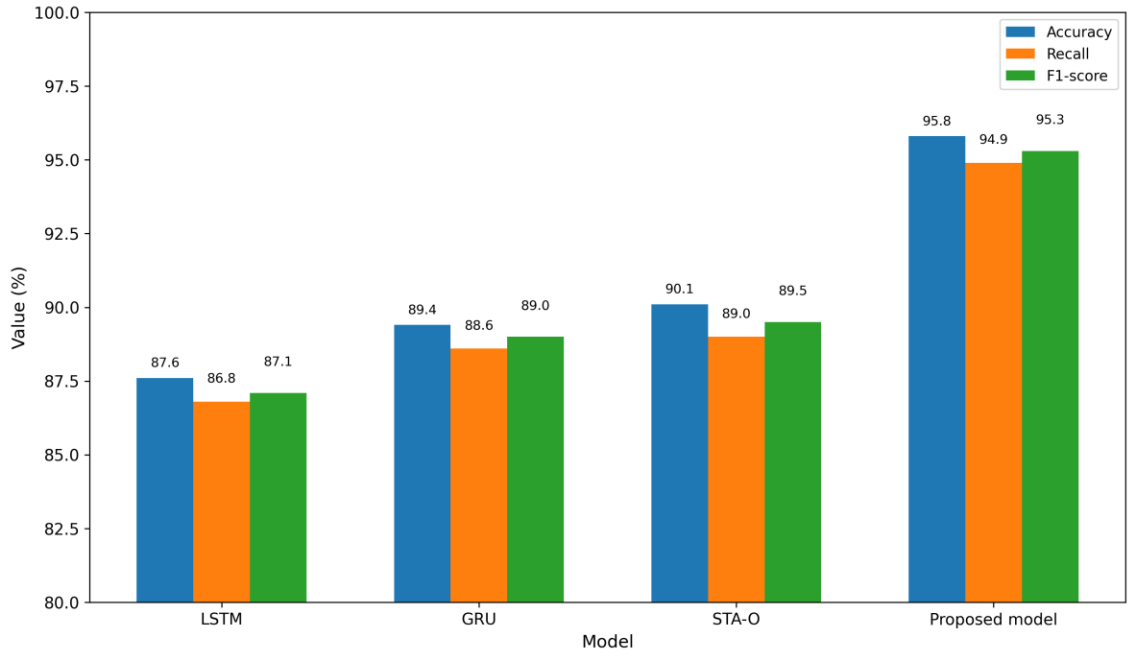


*Figure 7: Comparison of performance indicators of different algorithms*

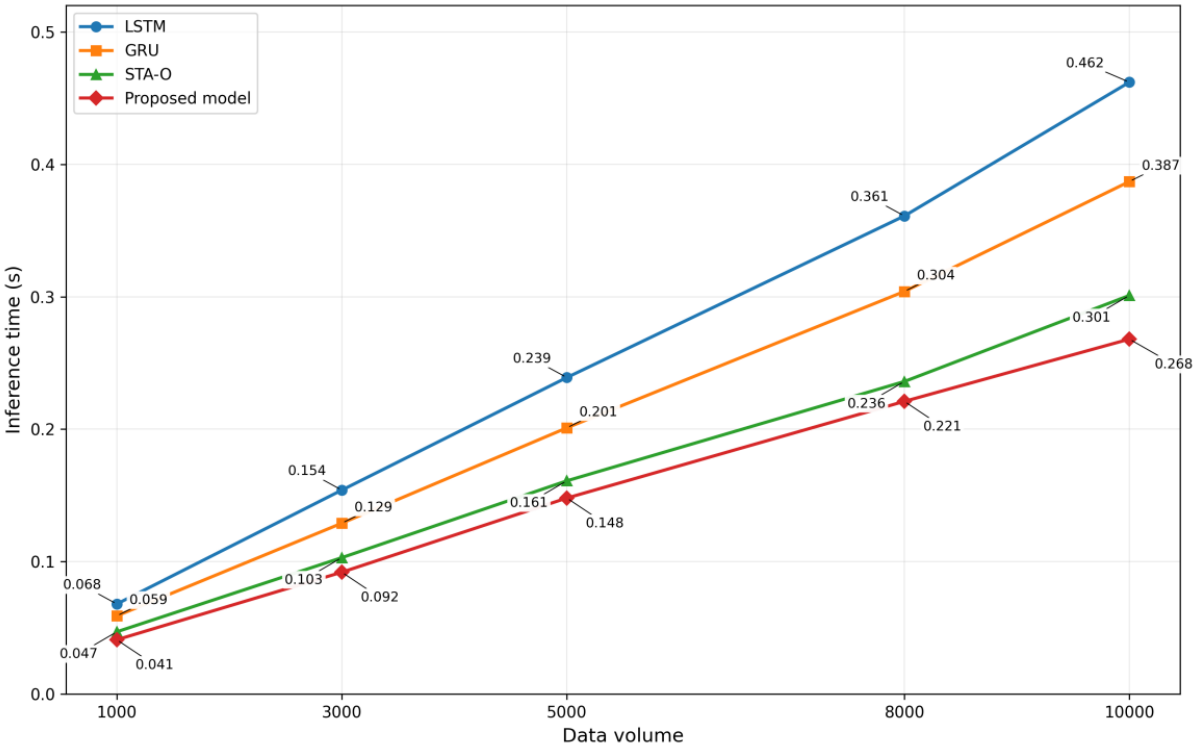


*Figure 8: Comparison plots of reasoning time of algorithms under different data scales*

In terms of prediction error and real-time reasoning ability, the proposed model also shows good comprehensive performance. The test results show that the RMSE and MAE of the proposed model are 0.118 and 0.074, which are lower than 0.196 and 0.131 of LSTM and 0.173 and 0.109 of GRU. At the same time, the edge-side deployment model can maintain stable inference efficiency in inference tests under different data scales. As shown in Figure 8, when the input scale increases from 1000 to 10000, the inference time of the proposed model increases from 0.041 s to 0.268 s. Compared with the unimproved spatio-temporal fusion model, the inference overhead of the proposed model is slightly increased under small-scale samples, but with the expansion of data scale, the growth rate is still relatively gentle. Compared with the inference time of 0.462 s of LSTM under 10000 data and 0.387 s of GRU, the proposed model still has more obvious real-time advantages in large-scale continuous monitoring data processing. This shows that the deployment method of combining edge-side lightweight reasoning and cloud parameter update not only improves the ability of the model to extract erosion evolution features, but also makes it better adapt to the application requirements of both timeliness and accuracy in real-time warning scenarios.

# 5 Conclusion

Focusing on the problems of response lag, high pressure of data transmission and insufficient dynamic prediction ability in soil erosion monitoring, this paper constructs a real-time monitoring and dynamic prediction system supported by edge computing, and forms a complete technical link of "perception collection, edge processing, cloud collaboration and early warning feedback". The experimental results show that the system has good engineering applicability in continuous monitoring scenarios: the mean absolute error of rainfall measurement is 0.41 mm, the mean absolute error of soil moisture is 1.63%, and the mean absolute error of sediment concentration is 0.28 g/L. Under the action of the edge

collaboration mechanism, the average response time of the system is 1.12 s, which is 31.4% shorter than that of the traditional centralized processing method. During the continuous operation for 72 h, there is no program crash and continuous data loss, which shows that the system can meet the requirements of real-time monitoring in terms of acquisition accuracy, transmission stability and operation reliability.

At the algorithm level, the dynamic prediction model constructed in this paper enhances the fine-grained description ability of erosion evolution process through the optimization of time dimension weight, the fusion of spatial dimension erosion factors and the collaborative expression of multi-source monitoring data. The test results show that the Accuracy, Recall and F1 of the proposed model reach 95.8%, 94.9%and 95.3%respectively, and the RMSE and MAE are reduced to 0.118 and 0.074 respectively. The overall performance of the proposed model is significantly better than that of LSTM, GRU and the unimproved spatio-temporal fusion model. This indicates that the cloud-edge collaborative deployment not only improves the recognition ability of high-risk erosion events, but also takes into account the real-time reasoning requirements in large-scale continuous data processing scenarios.

It should be pointed out that although the experimental data in this paper cover typical slope and simulation enhanced scenes, the proportion of extreme erosion samples is still relatively limited, and the generalization performance under different regional geophysics conditions still needs to be further tested. The follow-up research can focus on cross-regional migration modeling, adaptive threshold update and multi-scale remote sensing information access, to further improve the adaptive ability of the system to the complex basin environment and the intelligent early warning level.

# Funding

Supported by the Science and Technology Project of State Grid Shaanxi Electric Power Co., Ltd. (Project No.: 5226KY25001W)

# References

[1] Fernández D, Adermann E, Pizzolato M, et al. Comparative analysis of machine learning algorithms for soil erosion modelling based on remotely sensed data[J]. Remote sensing, 2023, 15(2): 482.

[2] Su J, Tang R, Lin H. Simulation and Spatio-Temporal Analysis of Soil Erosion in the Source Region of the Yellow River Using Machine Learning Method[J]. Land, 2024, 13(9): 1456.

[3] Bouamrane A, Boutaghane H, Bouamrane A, et al. Soil erosion susceptibility prediction using ensemble hybrid models with multicriteria decision-making analysis: Case study of the Medjerda basin, northern Africa[J]. International Journal of Sediment Research, 2024, 39(6): 998-1014.

[4] Bhattacharya R K, Chatterjee N D, Das K. Modelling of soil erosion susceptibility incorporating sediment connectivity and export at landscape scale using integrated machine learning, InVEST-SDR and Fragstats[J]. Journal of Environmental Management, 2024, 353: 120164.

[5] Mokarram M, Pourghasemi H R, Tiefenbacher J P, et al. Mapping soil erosion

susceptibility: a comparison of neural networks and fuzzy-AHP techniques[J]. Environmental earth sciences, 2024, 83(19): 564.

[6] Sadia H, Sarkar S K, Haydar M. Soil erosion susceptibility mapping in Bangladesh[J]. Ecological Indicators, 2023, 156: 111182.

[7] Kulimushi L C, Bashagaluke J B, Prasad P, et al. Soil erosion susceptibility mapping using ensemble machine learning models: A case study of upper Congo river sub-basin[J]. Catena, 2023, 222: 106858.

[8] Huang D, Su L, Fan H, et al. Identification of topographic factors for gully erosion susceptibility and their spatial modelling using machine learning in the black soil region of Northeast China[J]. Ecological Indicators, 2022, 143: 109376.

[9] Liu C, Fan H, Jiang Y, et al. Gully erosion susceptibility assessment based on machine learning-A case study of watersheds in Tuquan County in the black soil region of Northeast China[J]. Catena, 2023, 222: 106798.

[10] Liu C, Fan H, Wang Y. Gully erosion susceptibility assessment using three machine learning models in the black soil region of Northeast China[J]. Catena, 2024, 245: 108275.

[11] Wang Z, Zhang G, Wang C, et al. Assessment of the gully erosion susceptibility using three hybrid models in one small watershed on the Loess Plateau[J]. Soil and Tillage Research, 2022, 223: 105481.

[12] Zhu P, Xu H, Zhou L, et al. Automatic mapping of gully from satellite images using asymmetric non-local LinkNet: A case study in Northeast China[J]. International Soil and Water Conservation Research, 2024, 12(2): 365-378.

[13] Zhang S, Guo M, Liu X, et al. Historical evolution of gully erosion and its response to land use change during 1968–2018 in the Mollisol region of Northeast China[J]. International Soil and Water Conservation Research, 2024, 12(2): 388-402.

[14] Huang D, Zhao X, Yin Z, et al. Utilizing geodetectors to identify conditioning factors for gully erosion risk in the black soil region of northeast China[J]. International Soil and Water Conservation Research, 2024, 12(4): 808-827.

[15] Gelete T B, Pasala P, Abay N G, et al. Integrated machine learning and geospatial analysis enhanced gully erosion susceptibility modeling in the Erer watershed in Eastern Ethiopia[J]. Frontiers in Environmental Science, 2024, 12: 1410741.

[16] Baiddah A, Krimissa S, Hajji S, et al. Head-cut gully erosion susceptibility mapping in semi-arid region using machine learning methods: insight from the high atlas, Morocco[J]. Frontiers in Earth Science, 2023, 11: 1184038.

[17] Were K, Kebeney S, Churu H, et al. Spatial prediction and mapping of gully erosion susceptibility using machine learning techniques in a degraded semi-arid region of Kenya[J]. Land, 2023, 12(4): 890.

[18] Premkumar S, Sigappi A N. IoT-enabled edge computing model for smart irrigation

system[J]. Journal of Intelligent Systems, 2022, 31(1): 632-650.

[19] Roostaei J, Wager Y Z, Shi W, et al. IoT-based edge computing (IoTEC) for improved environmental monitoring[J]. Sustainable computing: informatics and systems, 2023, 38: 100870.

[20] Dong M, Yu H, Sun Z, et al. Research on agricultural environmental monitoring Internet of Things based on edge computing and deep learning[J]. Journal of Intelligent Systems, 2024, 33(1): 20230114.

[21] Makondo N, Kobo H I, Mathonsi T E, et al. A review on edge computing in 5G-enabled IoT for agricultural applications: Opportunities and challenges[C]//2023 International Conference on Electrical, Computer and Energy Technologies (ICECET). IEEE, 2023: 1-6.